International Journal of Hydrogen Energy 174 (2025) 151333

Contents lists available at ScienceDirect

International Journal of Hydrogen Energy

journal homepage: www.elsevier.com/locate/he

High-efficiency thermoeconomic approach for multi-generation at Afyon biogas power Plant: Electricity, liquid hydrogen, liquid carbon dioxide and hot water

Muhammed Arslan

Afyon Kocatepe University, Department of Motor Vehicles and Transportation Technologies, Afyonkarahisar, Turkey

ARTICLE INFO

Keywords:
Biogas
Hydrogen
Liquefaction
Heating
Thermodynamic
Thermoeconomic

ABSTRACT

This study proposes a high-efficiency multi-generation model for the Afyon Biogas Power Plant (ABP), which has a 4000 kW electricity generation capacity. In addition to electricity production, the proposed model integrates energy systems for heating, carbon dioxide liquefaction, hydrogen production and liquefaction, and hot water production. A comprehensive thermodynamic and thermoeconomic analysis of the system was conducted in coordination with Engineering Equation Solver (EES) and Aspen Plus. The thermodynamic results indicate that the ABP's energy efficiency, exergy efficiency, and useful energy are 14.29 %, 12.52 %, and 4000 kW, respectively. With the proposed model, these values achieve 75.05 %, 93.45 %, and 21,013 kW. The highest exergy destructions occur in the combustion chamber and HEX-2. The thermoeconomic results indicate that the unit costs of electricity, hydrogen production, hydrogen liquefaction, liquid hydrogen, carbon dioxide liquefaction, and hot water are calculated as 65.7 $/MWh, 2.64 $/kg, 2.754 $/kg, 5.394 $/kg, 0.36 $/kg, and 2.358 $/MWh, respectively. The proposed system's total equipment purchase cost is 22,126,876 $. These findings demonstrate that the proposed multi-generation model significantly enhances ABP's efficiency and economic feasibility by effectively utilizing exhaust gas waste energy and integrating energy systems.

1. Introduction

Technology, population growth, and components that make human life more comfortable have resulted in a significant energy demand, with global energy consumption increasing tenfold in the twentieth century. Considering the global energy crisis, climate change, and environmental pollution, there is an urgent need for rapid, significant, and long-term changes that can accelerate the transition to a sustainable energy system [1–9]. The European Union aims to limit global warming to 2 °C by 2050 within the European Green Deal and the Paris Agreement framework. Therefore, it is necessary to move away from fossil fuels and promote clean, carbon-free, and efficient energy technologies [10,11]. Currently, fossil fuels and renewable energy sources account for 82 % and 7.5 %, respectively, in meeting energy needs in the industry [12].

In the agricultural sector, renewable energy produced from existing resources in developed countries is reducing the demand for fossil fuels. Among renewable energy sources, biofuels are the most preferred and have the fourth largest energy reserves globally [13]. Biogas can be obtained from various biomass sources, such as agricultural waste, animal manure, municipal solid waste, and wastewater sludge. Additionally, its use reduces dependence on fossil fuels and contributes to waste management.

In contrast to wind or solar energy, biogas resources are portable and available in both urban and rural areas at all times. They can be flexibly transformed into various bioenergy forms, including options such as ethanol, biodiesel, biogas, and biomethane. Although rich in carbon, it is not yet a fossil material. It is an efficient energy source, especially in reducing environmental impacts, including heat production and greenhouse gas emissions. It ranks fourth among renewable energy sources in electricity generation. Biogas can generate electricity in internal combustion engines, microturbines, or innovative fuel cell systems. Generally, it operates as cogeneration units by recovering heat and producing electricity. Biogas can be upgraded to biomethane by removing byproducts (carbon dioxide, ammonia, water, nitrogen, hydrogen sulfide, siloxanes, etc.) from its content. This process results in a clean gas with a high thermal value. For this purpose, cryogenic separation, membrane application, and physicochemical absorption or adsorption are used. Finally, its properties are similar to those of fossil natural gas, making it suitable for use in places where it is utilized [3,5,10,12,14–17].

E-mail address: muarslan@aku.edu.tr.

https://doi.org/10.1016/j.ijhydene.2025.151333
Received 26 March 2025; Received in revised form 26 August 2025; Accepted 1 September 2025
Available online 10 September 2025
0360-3199/

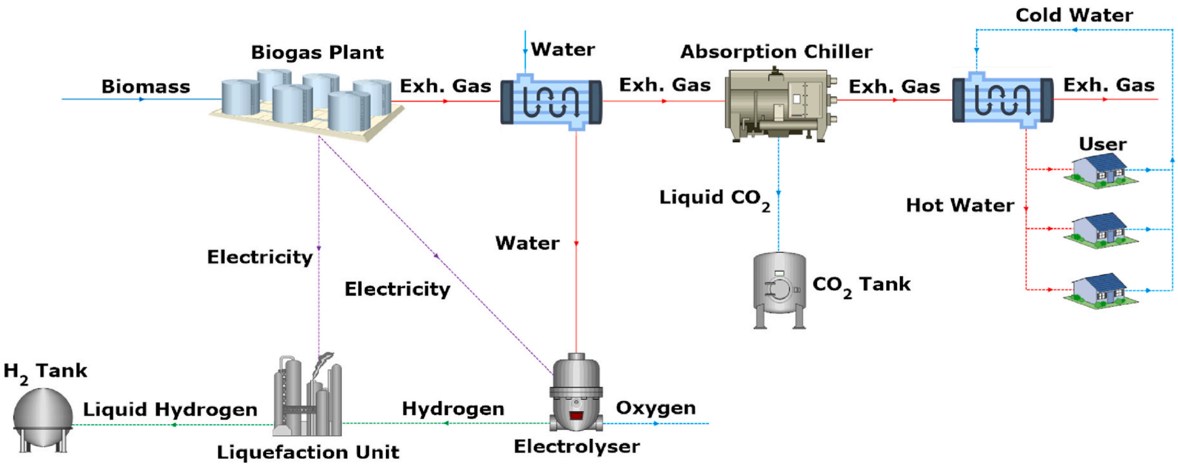

Fig. 1. Operation principle of proposed model.

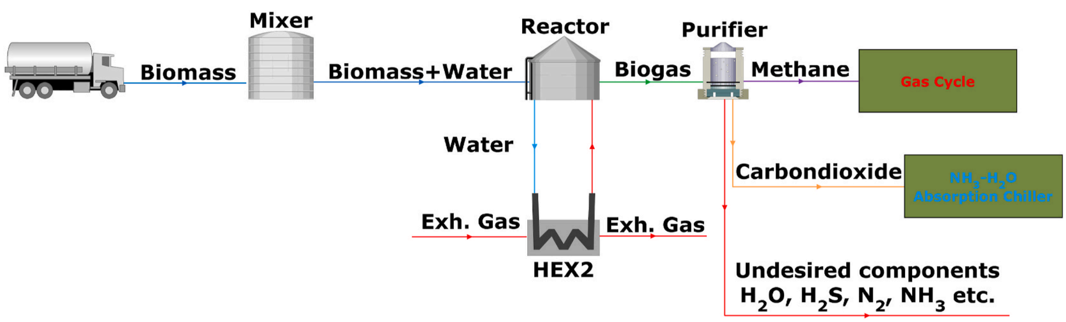

Fig. 2. Biogas production process.

Biogas is produced through the anaerobic digestion of organic matter in an oxygen-free environment. In this process, a large amount of carbon-based waste is utilized. This highlights the economic aspect of anaerobic digestion technology. Biological bacteria produce biogas through four chemical processes: hydrolysis, acidogenesis, acetogenesis, and methanogenesis. The methane content of biogas varies between 45 % and 75 %, depending on the raw materials used and the technique employed for biogas production; the remaining portion mainly consists of carbon dioxide and ammonia, carbon monoxide, halogenated hydrocarbons, hydrogen sulfide, nitrogen, siloxanes, and water vapor [2,3,11,18–20].

Moreover, reactors must be gas, water, and light impermeable. The composition of biogas is directly related to the digestion temperature, and as the temperature of the reactor where digestion occurs increases, the methane yield also increases. Therefore, heating the water mixed with biomass using exhaust gases and thermally insulating the reactor are effective methods. The digestion process is categorized based on reactor temperature. Mesophilic digestion occurs between 35 and 40 °C, providing balanced microbial activity and energy efficiency for biogas production. In contrast, thermophilic digestion occurs at higher temperatures, typically between 50 and 60 °C, resulting in faster decomposition and higher biogas yields but requiring more energy input for heating [14,21,22].

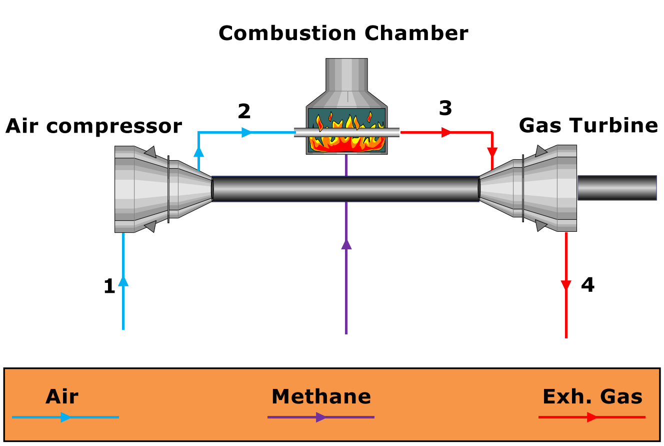

Fig. 3. Gas cycle process.

Scientists have conducted numerous studies on biogas technology, which has a high thermal value, is clean, and is still open to development. Some of these studies in the last five years in literature can be categorized as hybrid systems [23–38], thermodynamic and thermoeconomic analysis [4,39–47], biogas yield [2,48–56], green hydrogen [57–75], hydrogen storage [76–91], and electrolysis [92–102].

The study [103] by Ebadollahi et al. emphasized the importance of integrated energy systems (IES). IESs are specially designed systems that combine various energy sources to ensure low carbon emissions, reliability, and cost efficiency. Serving as an ideal solution for industries with high energy demand, IESs can be categorized based on the type and scope of by-products. They can integrate multiple energy processes to enhance efficiencies. The main purpose of this feasibility study is to propose a high-performance, environmentally friendly and sustainable hydrogen-focused model for the existing biogas power plant by combining hydrogen technology with IES technology. In this direction, the originality of the study is that the proposed model includes the complex process from biomass to hydrogen production and liquefaction, and supports this process with high thermodynamic performance thanks to heat recovery. The high thermodynamic efficiency enables increased hydrogen yield, promoting a shift toward carbon-free fuels. Another

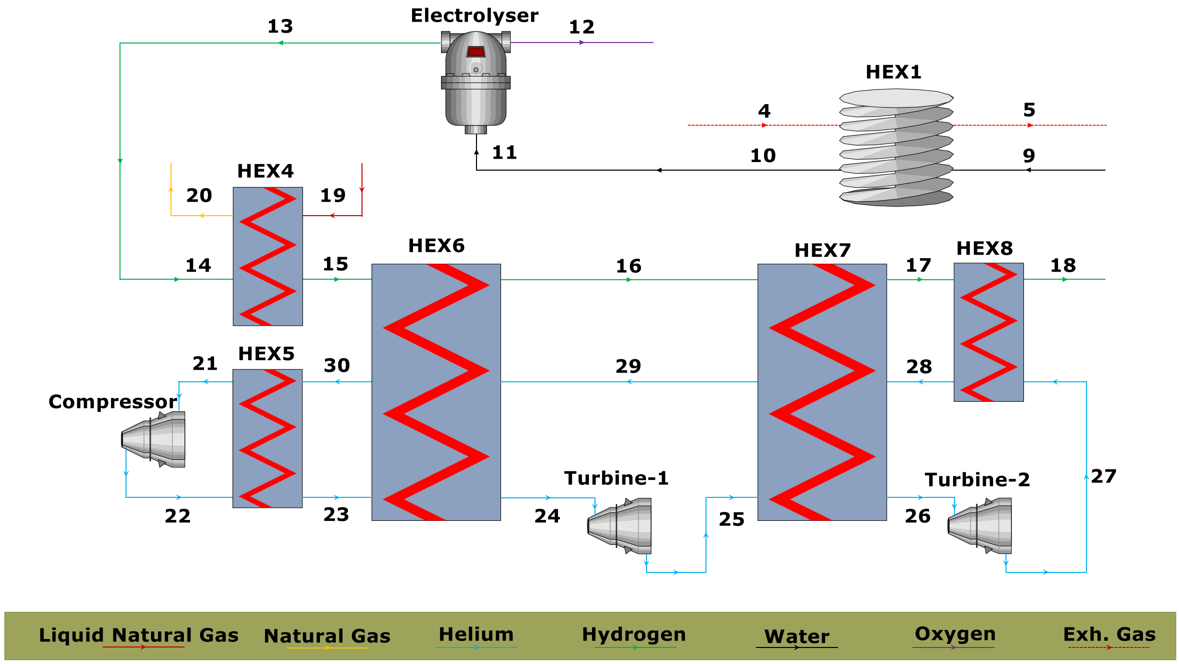

Fig. 4. Hydrogen production and liquefaction process.

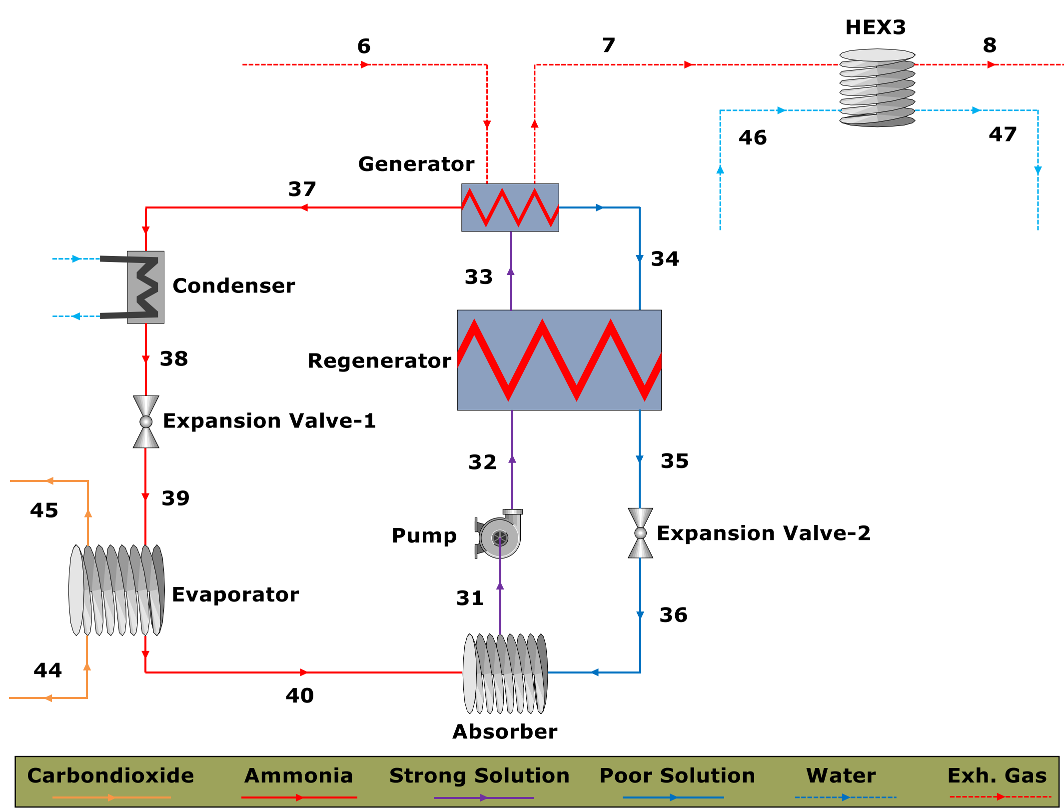

Fig. 5. Carbon dioxide liquefaction and hot water production process.

factor supporting the originality is that the biogas power plant produces the heat and electricity necessary for high efficiency in the hydrogen production and liquefaction process, with IES technology and does not require external heat or power. With the integration of energy systems into the ABP, a comprehensive model was designed involving the production of electricity, liquid carbon dioxide and hydrogen (both production and liquefaction), hot water, and heating. The model was analyzed thermodynamically and thermoeconomically, and important performance indicators were obtained. Since there is no dedicated software for designing a process consisting of such interdependent chemical and physical subprocesses while conducting thermodynamic and thermoeconomic analysis, a unique approach was developed using a coordinated simulation framework in EES and Aspen Plus. This method allows for a more precise and comprehensive evaluation of the system's performance and the numerical results of both software to verify each other. These features distinguish this study as a pioneering approach in

Table 1
Equations used in thermodynamic and thermoeconomic analysis.

Air Compressor	$\dot{m}_1 = \dot{m}_2$
	$\eta_{isen.} = \frac{h_{2s} - h_1}{h_2 - h_1}$
	$\dot{W}_{air\ compressor} = \dot{m}_1(h_2 - h_1)$
	$\dot{W}_{rev.,air\ compressor} = \dot{m}_1(ex_2 - ex_1)$
	$\dot{E}x_{dest.,air\ compressor} = \dot{W}_{air\ compressor} - \dot{W}_{rev.,air\ compressor}$ $c_1\dot{E}x_1 + c_{electricity}\dot{W}_{air\ compressor} + \dot{Z}_{air\ compressor} = c_2\dot{E}x_2$
Combustion Chamber (CC)	$\dot{m}_2 + \dot{m}_{biogas} = \dot{m}_3$
	$\dot{m}_2h_2 + \dot{m}_{methane}HV_{methane} = \dot{m}_3h_3$
	$\dot{E}x_{F,CC} = \dot{m}_{biogas}ex_{biogas}$
	$\dot{E}x_{P,CC} = \dot{m}_3ex_3 - \dot{m}_2ex_2$
	$\dot{E}x_{dest.,CC} = \dot{E}x_{F,CC} - \dot{E}x_{P,CC}$ $c_2\dot{E}x_2 + c_{biogas}\dot{m}_{biogas}ex_{biogas} + \dot{Z}_{CC} = c_3\dot{E}x_3$
Gas Turbine	$\dot{m}_3 = \dot{m}_4$
	$\eta_{isen.} = \frac{h_3 - h_4}{h_3 - h_{4s}}$
	$\dot{W}_{gas\ turbine} = \dot{m}_3(h_3 - h_4)$
	$\dot{W}_{rev.,gas\ turbine} = \dot{m}_3(ex_3 - ex_4)$
	$\dot{E}x_{dest.,gas\ turbine} = \dot{W}_{rev.,gas\ turbine} - \dot{W}_{gas\ turbine}$ $c_3\dot{E}x_3 + \dot{Z}_{gas\ turbine} = c_4\dot{E}x_4 + c_{electricity}\dot{W}_{gas\ turbine}$
HEX-1	$\dot{m}_4 = \dot{m}_5$
	$\dot{m}_9 = \dot{m}_{10}$
	$\dot{Q}_{HEX-1} = \dot{m}_4(h_4 - h_5) = \dot{m}_9(h_{10} - h_9)$
	$\dot{E}x_{dest.,HEX-1} = \dot{m}_4(ex_4 - ex_5) - \dot{m}_9(ex_{10} - ex_9)$ $c_4\dot{E}x_4 + c_9\dot{E}x_9 + \dot{Z}_{HEX-1} = c_5\dot{E}x_5 + c_{10}\dot{E}x_{10}$
HEX-2	$\dot{m}_5 = \dot{m}_6$
	$\dot{Q}_{HEX-2} = \dot{m}_5(h_5 - h_6) = \dot{m}_{reactor\ feed\ water}(h_o - h_i)$
	$\dot{E}x_{dest.,HEX-2} = \dot{m}_5(ex_5 - ex_6) - \dot{m}_{reactor\ feed\ water}(ex_o - ex_i)$ $c_5\dot{E}x_5 + c_i\dot{E}x_i + \dot{Z}_{HEX-2} = c_6\dot{E}x_6 + c_o\dot{E}x_o$
HEX-3	$\dot{m}_7 = \dot{m}_8$
	$\dot{m}_{46} = \dot{m}_{47}$
	$\dot{Q}_{HEX-3} = \dot{m}_7(h_7 - h_8) = \dot{m}_{46}(h_{47} - h_{46})$
	$\dot{E}x_{dest.,HEX-3} = \dot{m}_7(ex_7 - ex_8) - \dot{m}_{46}(ex_{47} - ex_{46})$ $c_7\dot{E}x_7 + c_{46}\dot{E}x_{46} + \dot{Z}_{HEX-3} = c_8\dot{E}x_8 + c_{47}\dot{E}x_{47}$
Electrolyser	$\dot{m}_{10} = \dot{m}_{11}$
	$\dot{m}_{11} = \dot{m}_{12} + \dot{m}_{13}$
	$\dot{E}x_{F,electrolyser} = \dot{m}_{11}ex_{11} + \dot{W}_{electrolysis}$
	$\dot{E}x_{P,electrolyser} = \dot{m}_{12}ex_{12} + \dot{m}_{13}ex_{13}$
	$\dot{E}x_{dest.,electrolyser} = \dot{E}x_{F,electrolyser} - \dot{E}x_{P,electrolyser}$
	$\eta_{en} = \frac{\dot{m}_{13}HV_{H_2}}{\dot{W}_{electrolysis}}$
	$\eta_{ex} = \frac{\dot{m}_{13}ex_{H_2}}{\dot{W}_{electrolysis}}$ $c_{11}\dot{E}x_{11} + c_{electricity}\dot{W}_{electrolysis} + \dot{Z}_{electrolyser} = c_{12}\dot{E}x_{12} + c_{13}\dot{E}x_{13}$
HEX-4	$\dot{m}_{13} = \dot{m}_{14} = \dot{m}_{15}$
	$\dot{m}_{19} = \dot{m}_{20}$
	$\dot{Q}_{HEX-4} = \dot{m}_{14}(h_{14} - h_{15}) = \dot{m}_{19}(h_{20} - h_{19})$
	$\dot{E}x_{dest.,HEX-4} = \dot{m}_{14}(ex_{14} - ex_{15}) - \dot{m}_{19}(ex_{20} - ex_{19})$ $c_{14}\dot{E}x_{14} + c_{19}\dot{E}x_{19} + \dot{Z}_{HEX-4} = c_{15}\dot{E}x_{15} + c_{20}\dot{E}x_{20}$
HEX-5	$\dot{m}_{21} = \dot{m}_{30}$
	$\dot{m}_{22} = \dot{m}_{23}$
	$\dot{Q}_{HEX-5} = \dot{m}_{21}(h_{21} - h_{30}) = \dot{m}_{22}(h_{22} - h_{23})$
	$\dot{E}x_{dest.,HEX-5} = \dot{m}_{21}(ex_{21} - ex_{30}) - \dot{m}_{22}(ex_{22} - ex_{23})$ $c_{22}\dot{E}x_{22} + c_{30}\dot{E}x_{30} + \dot{Z}_{HEX-5} = c_{21}\dot{E}x_{21} + c_{23}\dot{E}x_{23}$
HEX-6	$\dot{m}_{15} = \dot{m}_{16}$
	$\dot{m}_{23} = \dot{m}_{24}$
	$\dot{m}_{29} = \dot{m}_{30}$
	$\dot{Q}_{HEX-6} = \dot{m}_{15}(h_{15} - h_{16}) + \dot{m}_{23}(h_{23} - h_{24}) = \dot{m}_{29}(h_{30} - h_{29})$
	$\dot{E}x_{dest.,HEX-6} = \dot{m}_{15}(ex_{15} - ex_{16}) + \dot{m}_{23}(ex_{23} - ex_{24}) - \dot{m}_{29}(ex_{30} - ex_{29})$ $c_{15}\dot{E}x_{15} + c_{23}\dot{E}x_{23} + c_{29}\dot{E}x_{29} + \dot{Z}_{HEX-6} = c_{16}\dot{E}x_{16} + c_{24}\dot{E}x_{24} + c_{30}\dot{E}x_{30}$
HEX-7	$\dot{m}_{16} = \dot{m}_{17}$
	$\dot{m}_{28} = \dot{m}_{29}$
	$\dot{m}_{25} = \dot{m}_{26}$
	$\dot{Q}_{HEX-7} = \dot{m}_{16}(h_{16} - h_{17}) + \dot{m}_{25}(h_{25} - h_{26}) = \dot{m}_{28}(h_{29} - h_{28})$
	$\dot{E}x_{dest.,HEX-7} = \dot{m}_{16}(ex_{16} - ex_{17}) + \dot{m}_{25}(ex_{25} - ex_{26}) - \dot{m}_{28}(ex_{29} - ex_{28})$ $c_{16}\dot{E}x_{16} + c_{25}\dot{E}x_{25} + c_{28}\dot{E}x_{28} + \dot{Z}_{HEX-7} = c_{17}\dot{E}x_{17} + c_{26}\dot{E}x_{26} + c_{29}\dot{E}x_{29}$
HEX-8	$\dot{m}_{17} = \dot{m}_{18}$
	$\dot{m}_{27} = \dot{m}_{28}$
	$\dot{Q}_{HEX-8} = \dot{m}_{17}(h_{17} - h_{18}) = \dot{m}_{27}(h_{28} - h_{27})$
	$\dot{E}x_{dest.,HEX-8} = \dot{m}_{17}(ex_{17} - ex_{18}) - \dot{m}_{27}(ex_{28} - ex_{27})$ $c_{17}\dot{E}x_{17} + c_{27}\dot{E}x_{27} + \dot{Z}_{HEX-8} = c_{18}\dot{E}x_{18} + c_{28}\dot{E}x_{28}$
Compressor	$\dot{m}_{21} = \dot{m}_{22}$
	$\dot{Q}_{compressor} = \dot{W}_{compressor} = \dot{m}_1RT_1 \ln\left(\frac{P_1}{P_2}\right)$
	$\dot{W}_{compressor} = \dot{m}_1(h_2 - h_1)$
	$\dot{W}_{rev.,compressor} = \dot{m}_1(ex_2 - ex_1)$
	$\dot{E}x_{dest.,compressor} = \dot{W}_{compressor} - \dot{W}_{rev.,compressor}$ $c_{21}\dot{E}x_{21} + c_{electricity}\dot{W}_{compressor} + \dot{Z}_{compressor} = c_{22}\dot{E}x_{22}$
Turbine-1	$\dot{m}_{24} = \dot{m}_{25}$
	$\eta_{isen.} = \frac{h_{24} - h_{25}}{h_{24} - h_{25s}}$
	$\dot{W}_{turbine-1} = \dot{m}_{24}(h_{24} - h_{25})$

(*continued on next page*)

Table 1 (*continued*)

	$\dot{W}_{rev.,turbine-1} = \dot{m}_{24}(ex_{24} - ex_{25})$
	$\dot{E}x_{dest.,turbine-1} = \dot{W}_{rev.,turbine-1} - \dot{W}_{turbine-1}$ $c_{24}\dot{E}x_{24} + \dot{Z}_{turbine-1} = c_{25}\dot{E}x_{25} + c_{electricity}\dot{W}_{turbine-1}$
Turbine-2	$\dot{m}_{26} = \dot{m}_{27}$
	$\eta_{isen.} = \dfrac{h_{26} - h_{27}}{h_{26} - h_{27s}}$
	$\dot{W}_{turbine-2} = \dot{m}_{26}(h_{26} - h_{27})$
	$\dot{W}_{rev.,turbine-2} = \dot{m}_{26}(ex_{26} - ex_{27})$
	$\dot{E}x_{dest.,turbine-2} = \dot{W}_{rev.,turbine-2} - \dot{W}_{turbine-2}$
Pump	$\dot{m}_{31} = \dot{m}_{32}$
	$h_{31} \cong h_{32}$
	$\dot{W}_{pump} = \dot{m}_{31}(h_{32} - h_{31})$
	$\dot{W}_{rev.,pump} = \dot{m}_{31}(ex_{32} - ex_{31})$
	$\dot{E}x_{dest.,pump} = \dot{W}_{rev.,pump} - \dot{W}_{pump}$ $c_{31}\dot{E}x_{31} + c_{electricity}\dot{W}_{pump} + \dot{Z}_{pump} = c_{32}\dot{E}x_{32}$
Regenerator	$\dot{m}_{32} = \dot{m}_{33}$
	$\dot{m}_{34} = \dot{m}_{35}$
	$\dot{Q}_{regenerator} = \dot{m}_{32}(h_{33} - h_{32}) = \dot{m}_{34}(h_{34} - h_{35})$
	$\dot{E}x_{dest.,regenerator} = \dot{m}_{32}(ex_{33} - ex_{32}) - \dot{m}_{34}(ex_{34} - ex_{35})$ $c_{32}\dot{E}x_{32} + c_{34}\dot{E}x_{34} + \dot{Z}_{regenerator} = c_{33}\dot{E}x_{33} + c_{35}\dot{E}x_{35}$
Generator	$\dot{m}_{33} = \dot{m}_{34} + \dot{m}_{37}$
	$\dot{m}_{6} = \dot{m}_{7}$
	$\dot{Q}_{generator} = \dot{m}_{34}h_{34} + \dot{m}_{37}h_{37} - \dot{m}_{33}h_{33} = \dot{m}_{6}(h_{6} - h_{7})$
	$\dot{E}x_{dest.,generator} = \dot{m}_{34}ex_{34} + \dot{m}_{37}ex_{37} - \dot{m}_{33}ex_{33}$ $c_{33}\dot{E}x_{33} + \dot{Z}_{generator} = c_{34}\dot{E}x_{34} + c_{37}\dot{E}x_{37}$
Expansion Valve-2	$\dot{m}_{35} = \dot{m}_{36}$
	$h_{35} \cong h_{36}$
	$\dot{E}x_{F,expansion\ valve-2} = \dot{m}_{35}h_{35}$
	$\dot{E}x_{P,expansion\ valve-2} = \dot{m}_{36}h_{36}$
	$\dot{E}x_{dest.,expansion\ valve-2} = \dot{E}x_{F,expansion\ valve-2} - \dot{E}x_{P,expansion\ valve-2}$ $c_{35}\dot{E}x_{35} + \dot{Z}_{expansion\ valve-2} = c_{36}\dot{E}x_{36}$
Condenser	$\dot{m}_{37} = \dot{m}_{38}$
	$\dot{Q}_{condenser} = \dot{m}_{37}(h_{37} - h_{38}) = \dot{m}_{condenser}(h_{o} - h_{i})$
	$\dot{E}x_{dest.,condenser} = \dot{m}_{37}(ex_{37} - ex_{38}) - \dot{m}_{condenser}(ex_{o} - ex_{i})$ $c_{37}\dot{E}x_{37} + c_{i}\dot{E}x_{i} + \dot{Z}_{condenser} = c_{38}\dot{E}x_{38} + c_{o}\dot{E}x_{o}$
Expansion Valve-1	$\dot{m}_{38} = \dot{m}_{39}$
	$h_{38} \cong h_{39}$
	$\dot{E}x_{F,expansion\ valve-1} = \dot{m}_{38}h_{38}$
	$\dot{E}x_{P,expansion\ valve-1} = \dot{m}_{39}h_{39}$
	$\dot{E}x_{dest.,expansion\ valve-1} = \dot{E}x_{F,expansion\ valve-1} - \dot{E}x_{P,expansion\ valve-1}$ $c_{38}\dot{E}x_{38} + \dot{Z}_{expansion\ valve-1} = c_{39}\dot{E}x_{39}$
Evaporator	$\dot{m}_{39} = \dot{m}_{40}$
	$\dot{m}_{44} = \dot{m}_{45}$
	$\dot{Q}_{evaporator} = \dot{m}_{39}(h_{40} - h_{39}) = \dot{m}_{44}(h_{44} - h_{45})$
	$\dot{E}x_{dest.,evaporator} = \dot{m}_{39}(ex_{40} - ex_{39}) - \dot{m}_{44}(ex_{44} - ex_{45})$ $c_{39}\dot{E}x_{39} + c_{44}\dot{E}x_{44} + \dot{Z}_{evaporator} = c_{40}\dot{E}x_{40} + c_{45}\dot{E}x_{45}$
Absorber	$\dot{m}_{31} = \dot{m}_{36} + \dot{m}_{40}$
	$\dot{Q}_{absorber} = \dot{m}_{36}h_{36} + \dot{m}_{40}h_{40} - \dot{m}_{31}h_{31}$
	$\dot{E}x_{dest.,absorber} = \dot{m}_{36}ex_{36} + \dot{m}_{40}ex_{40} - \dot{m}_{31}ex_{31}$ $c_{36}\dot{E}x_{36} + c_{40}\dot{E}x_{40} + \dot{Z}_{absorber} = c_{31}\dot{E}x_{31}$
ABP	$\dot{W}_{net} = \dot{W}_{gas\ turbine} - \dot{W}_{air\ compressor}$
	$\eta_{en} = \dfrac{\dot{W}_{net}}{\dot{m}_{methane}HV_{methane}}$
	$\eta_{ex} = \dfrac{\dot{W}_{net}}{\dot{m}_{methane}ex_{methane}}$
Proposed Model	$\eta_{en} = \dfrac{\dot{W}_{net} + \dot{Q}_{HEX-1} + \dot{Q}_{HEX-2} + \dot{Q}_{HEX-3} + \dot{Q}_{regenerator}}{\dot{m}_{methane}HV_{methane}}$
	$\eta_{ex} = \dfrac{\dot{W}_{net} + \dot{E}x_{HEX-1} + \dot{E}x_{HEX-2} + \dot{E}x_{HEX-3} + \dot{E}x_{regenerator}}{\dot{m}_{methane}ex_{methane}}$

hydrogen production design, demonstrating the feasibility of utilizing waste heat in biogas power plants for cost-effective and sustainable multi-generation.

2. Operation principle of proposed model

Fig. 1 presents the operating principle of the proposed model for ABP. The model integrates various energy systems into the existing plant to utilize the exhaust gas waste energy. Biogas is produced from biomass and purified from undesirable substances in a bio-claner. After the purification process, the methane gas obtained is sent to the combustion chamber.

The exhaust gas leaving the gas cycle is utilized in a heat exchanger for heating water to 80 °C in order to improve electrolysis efficiency. The dual-turbine reverse Brayton cycle represents the liquefaction unit, and the hydrogen produced via electrolysis is liquefied in this liquefaction unit. The powers required for the helium compressor in the reverse Brayton cycle and required for electrolysis are supplied by the electricity generated in the gas cycle.

The still high-energy exhaust gas is used to heat the reactor feed water to enhance methane yield.

Then, exhaust gas waste energy is utilized for the liquefaction of carbon dioxide. The ammonia-water absorption chiller unit represents the liquefaction unit of carbon dioxide. Finally, the exhaust gas heats cold water in a heat exchanger before being released into the atmosphere. Consequently, low-energy exhaust gas is released into the atmosphere to reduce environmental harm.

2.1. - Biogas production

Fig. 2 presents the biogas production process. The collected biomass is into smaller pieces in the plant mixer and mixed with water. It is then sent to the reactor for the digestion process. Biogas is produced by chemical bacteria from the biomass, which is kept at 35–40 °C. At this stage, the biogas is not suitable for use in the gas cycle due to its composition. Most carbon dioxide by-products are sent to an ammonia-

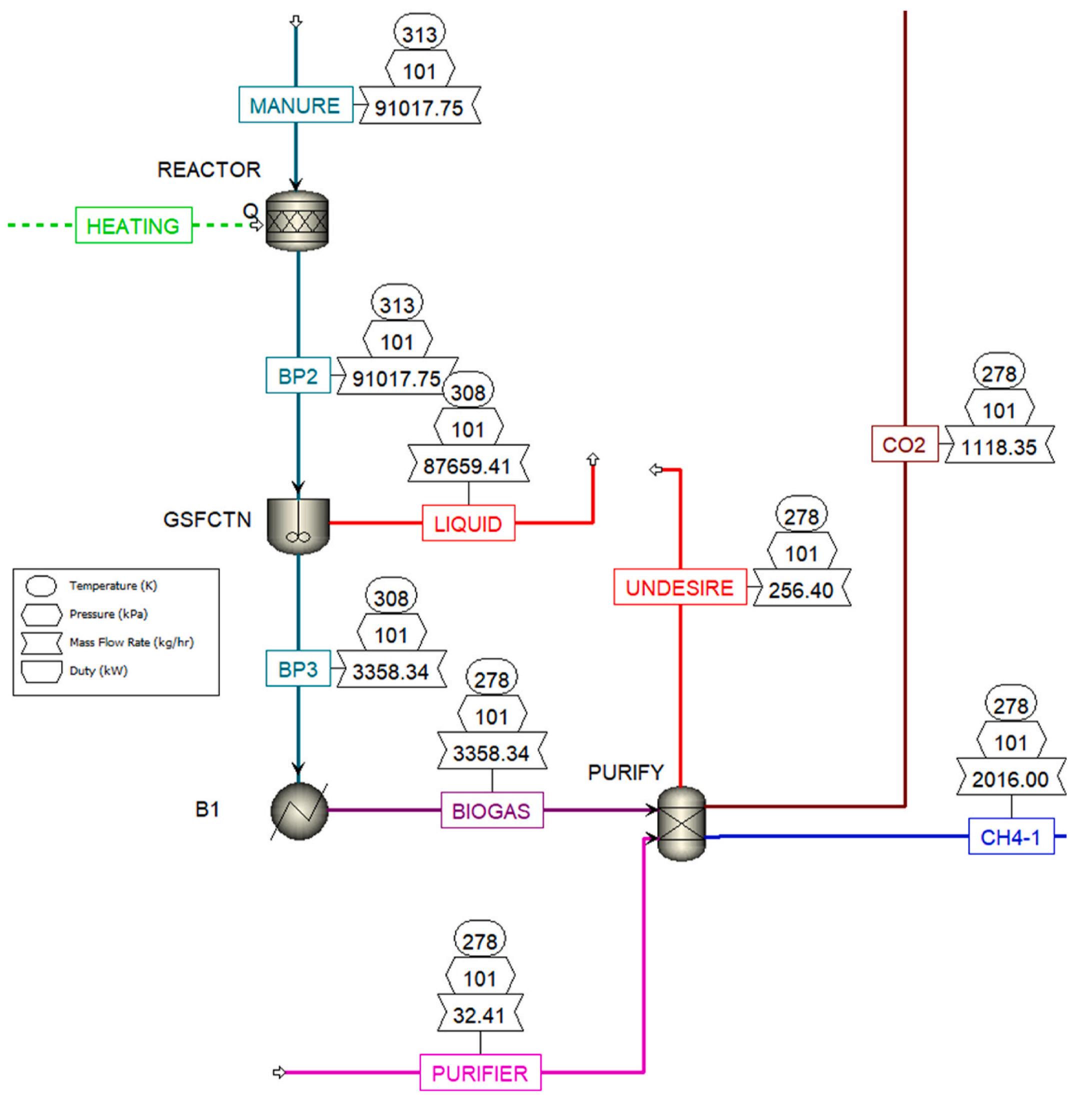

Fig. 6. Biogas production process designed by Aspen Plus.

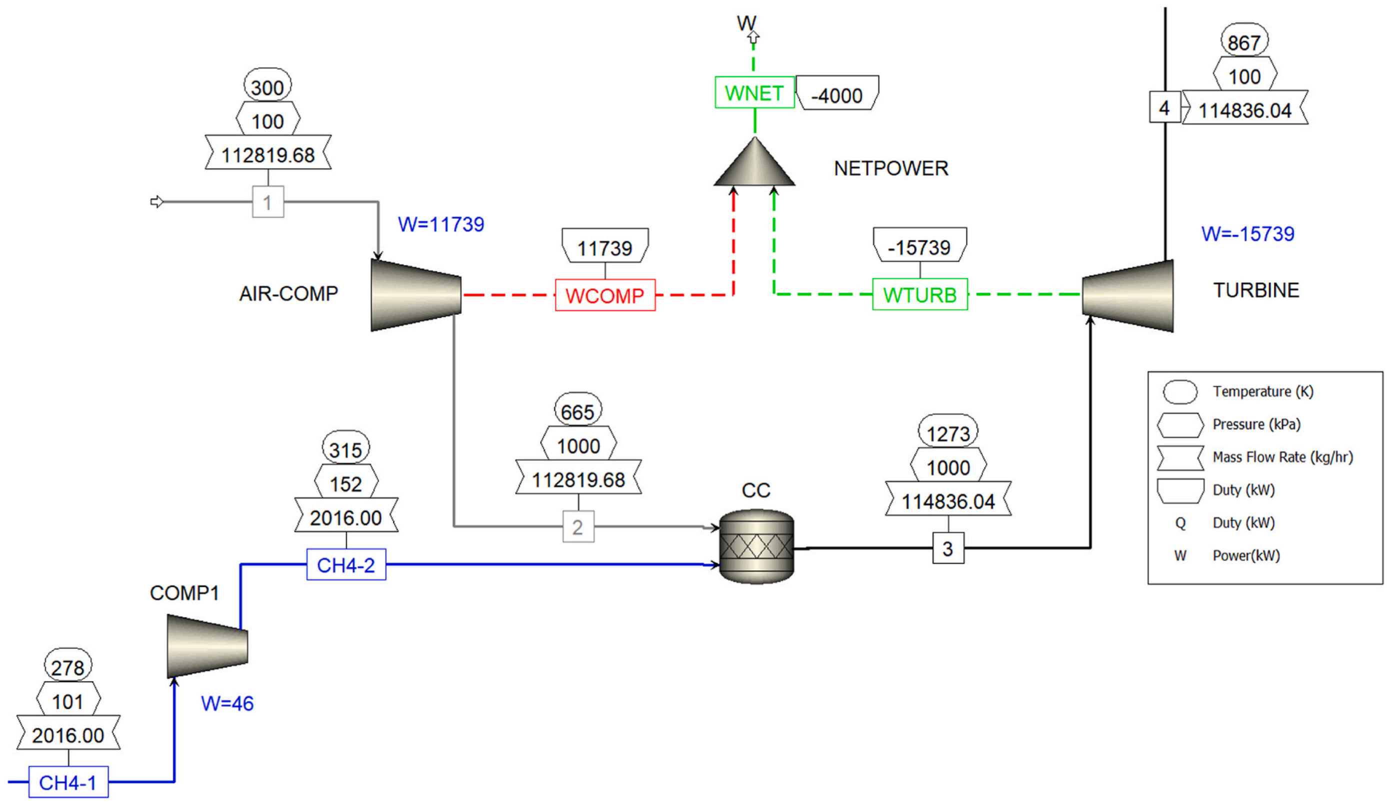

Fig. 7. Gas cycle designed by Aspen Plus.

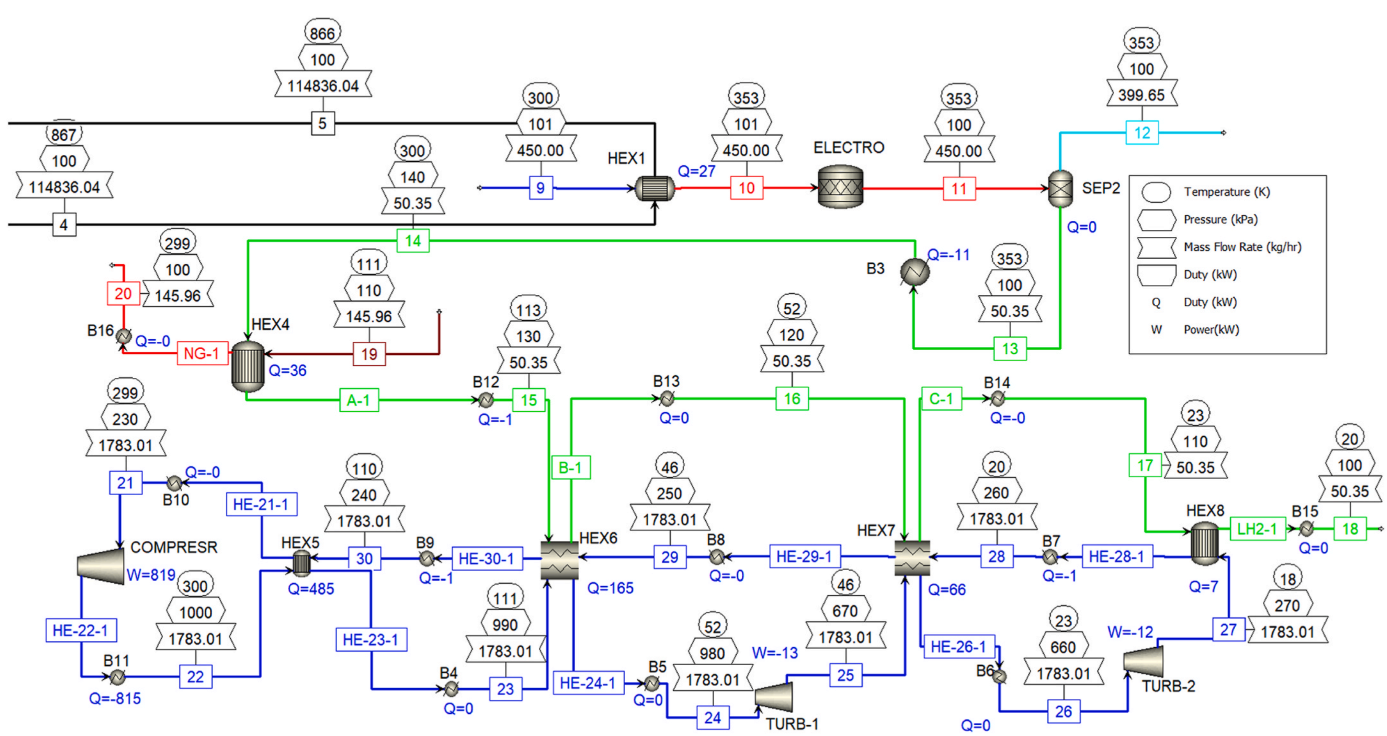

Fig. 8. Hydrogen production and liquefaction unit with reverse Brayton cycle designed by Aspen Plus.

water absorption chiller unit for liquefaction. At the same time, water is separated from the biogas using a cyclone separator. Hydrogen sulfide is also decomposed into hydrogen and sulfur by sulfide bacteria to prevent corrosion and wearing, and sulfur is used to enhance fertilizer yield. The trace amount of ammonia first dissolves in water and then reacts with air. So, it is converted into nitrogen and released into the atmosphere.

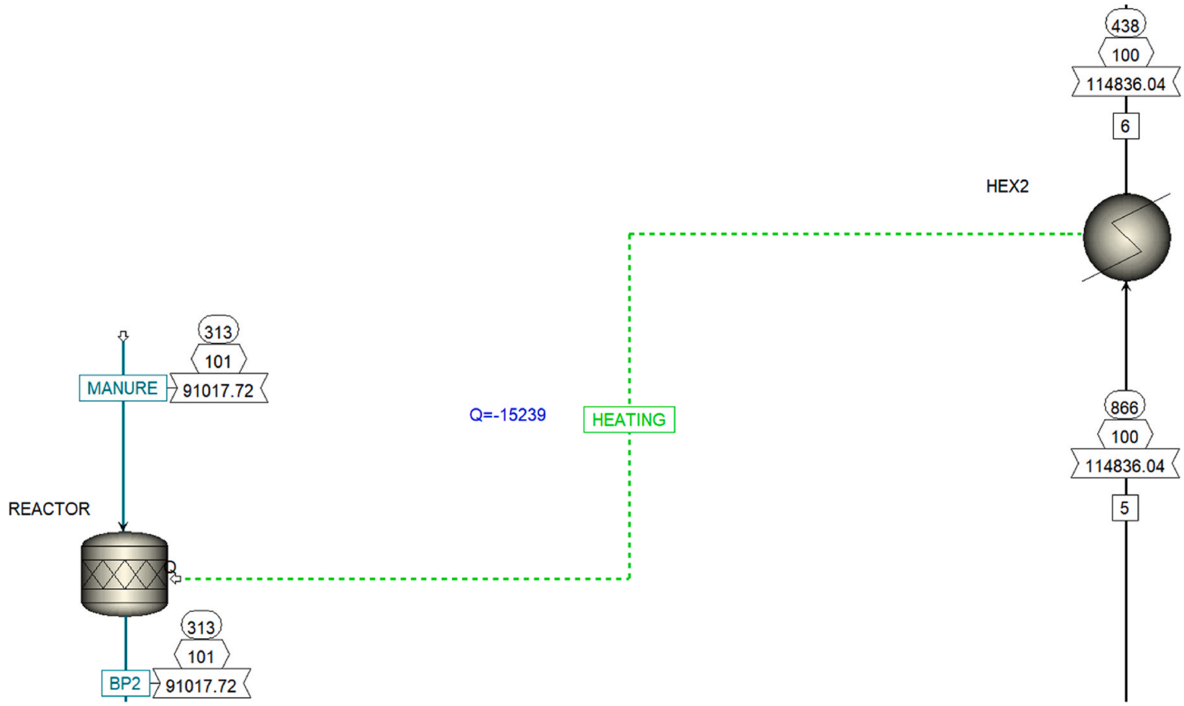

Fig. 9. Reactor heating unit designed by Aspen plus.

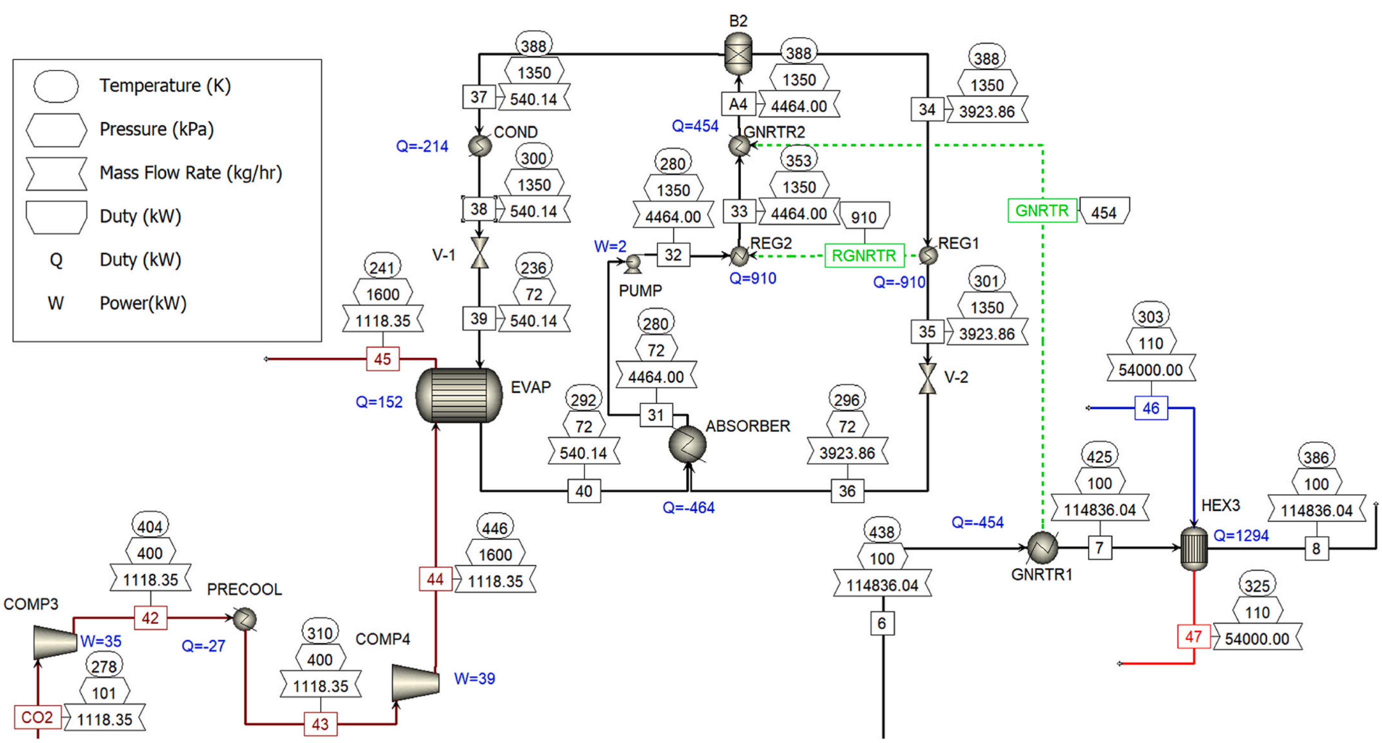

Fig. 10. Carbon dioxide liquefaction and hot water production units designed by Aspen plus.

After purification, the methane is sent to the combustion chamber.

2.2. - Gas cycle

Fig. 3 presents the gas cycle process. Atmospheric air is compressed in the compressor and reacts with the methane gas in the combustion chamber. The high-energy exhaust gas released drives the gas turbine. The gas turbine supplies the required compressor power, while the remaining shaft power is converted into electrical energy.

2.3. - Production and liquefaction of hydrogen

Fig. 4 presents the production and liquefaction of the hydrogen process. The preheated water is converted into oxygen and hydrogen in the electrolyzer. The produced hydrogen is sent to the liquefaction unit. In the liquefaction unit, hydrogen is pre-cooled with Liquid Natural Gas

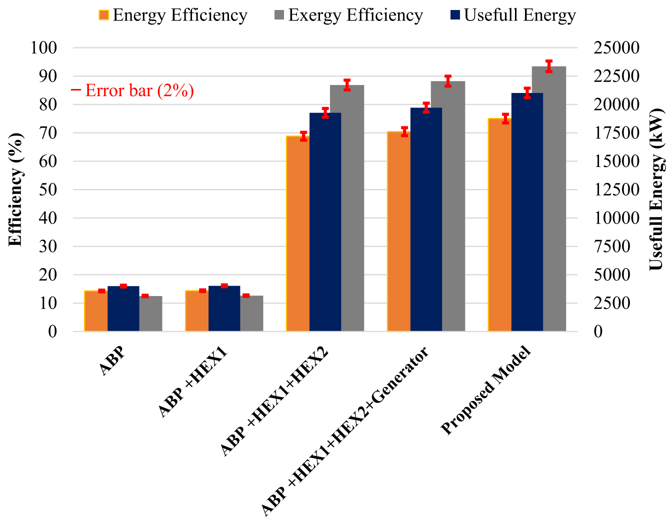

Fig. 11. Thermodynamic performance of ABP and proposed model.

(LNG) and then chiefly cooled by helium in a cascade manner to 20 K. The pressurized helium is expanded in two turbines, providing cooling and power generation.

2.4. - Liquefaction of carbon dioxide and production of hot water

Fig. 5 presents the liquefaction of carbon dioxide and the production of the hot water process. The exhaust gas waste energy is used in the generator of the absorption chiller to separate the ammonia-water solution. The fluid, which is cooled in the condenser and expanded at the expansion valve, liquefies carbon dioxide in the evaporator. Finally, the exhaust gas heats the cold water in the heating unit for hot water production. It is then released into the atmosphere in a low-energy state.

3. Thermodynamic and thermoeconomic analysis

A comprehensive and realistic analysis is required to calculate the detailed thermodynamic performance and product costs of the existing plant and the proposed model. This section presents the equations necessary for thermodynamic and thermoeconomic analysis at the equipment and plant levels. The equations provided in Table 1 include the mass flow rate, shaft power, thermal power, energy and exergy efficiencies, and exergy destructions. The results of the thermodynamic analysis represent the foundation of the thermoeconomic analysis and are combined with economic data to complete the thermoeconomic analysis. The thermoeconomic analysis equations include unit flow cost, exergy cost ratio, equipment cost ratio, and total equipment purchase cost.[1]

The detailed assumptions required for the analysis are provided in the following [104–112].

- The heat value of biogas is 30,000 kJ/kg.
- Isentropic efficiencies of the compressor and turbine are 75 %.
- There is no pressure drop in the exhaust gas line.
- Biogas composition is as follows: methane - 60 %, carbon dioxide - 33 %, water - 4.7 % and others (ammonia, nitrogen, hydrogen, oxygen, hydrogen sulfide, etc.) - 2.3 %.
- The reactors are lined with a high-density polyethylene membrane.
- The total reactor capacity is 236,286 m^3.
- Anaerobic fermentation is carried out at 35 °C for 30 days.
- The composition of atmospheric air is 21 % oxygen and 79 % nitrogen.
- The proposed model is assumed to operate for 7884 h per year.
- Interest rate and operation and maintenance correction factor are 6 % and 1.06, respectively.
- There is no leakage in the system.
- Temperature range, degradation rate, and efficiency at partial load of proton exchange membrane (PEM) electrolyzer are 50–80 °C, 5 μV/h, and 75 %, respectively.

3.1. - Steps of analysis

1. Designing biogas production with Aspen Plus and determining the amount and composition of biogas produced.
2. Analyzing the EES combustion reaction and transferring the results to Aspen Plus.
3. Integrating energy systems into ABP using the model designed by Aspen Plus.
4. Thermodynamic analysis using Aspen Plus and EES.
5. Thermoeconomic analysis based on current equipment costs from the Aspen Plus database and exergy data obtained from EES.

4. Results and discussion

In the model designed by Aspen Plus, the biogas production process based on the plant's daily biomass input data is presented in Fig. 6. The mass flow rates of the produced biogas, methane, and carbon dioxide are determined as 3358.34 kg/h, 2016 kg/h, and 1118.35 kg/h, respectively.

In Fig. 7, the gas cycle process designed by Aspen Plus is presented. In the cycle, the compressor consumes 11,739 kW of power, while the turbine generates 15,739 kW of power, resulting in a net power output of 4000 kW. The high-energy exhaust gas drives the IESs after the turbine.

Fig. 8 presents the hydrogen production and reverse Brayton cycle hydrogen liquefaction unit designed by Aspen Plus. According to the results of the analysis, 50.35 kg/h of hydrogen is produced from 450 kg/h of water. The produced hydrogen is then sent to the liquefaction unit, pre-cooled to 113 K along HEX-4 using LNG. Subsequently, its temperature is gradually reduced to 52 K, 23 K, and finally 20 K. During this process, cold helium cools both the hydrogen and the hot helium. The plant supplies the required electrical power for hydrogen production and the helium compressor, 2200 kW and 819 kW, respectively.

Fig. 9 shows the reactor heating unit designed by Aspen Plus. With the integration of HEX-2, a significant part of exhaust gas is utilized to heat the reactor. As a result, the exhaust gas temperature drops significantly. The main reason for the proposed model's high efficiency is the heating reactor.

Before leaving the power plant, the final stage of exhaust gas energy integration consists of the carbon dioxide liquefaction and hot water production units. The exhaust gas drives the generator of the ammonia-water absorption chiller unit. After providing the necessary energy to separate the solution, the condensed to 236 K and expanded fluid cooled the carbon dioxide to 241 K, causing it to transition to the liquid phase under high pressure. Finally, the exhaust gas heats the cold water to 325 K through HEX-3 and is released into the atmosphere at 386 K. Fig. 10 presents the carbon dioxide liquefaction and hot water production units designed by Aspen Plus.

The IESs in the proposed model enhance the efficiency of ABP. Fig. 11 presents the IESs' contributions to ABP's thermodynamic performance. The plant's efficiency has reached remarkably high levels with the proposed model. The energy efficiency-exergy efficiency-useful energy of ABP and the proposed model are calculated as 14.29 %-12.52

[1] I have noticed layout issues in both the online preview and the proof PDF: several figures, tables, and headings are misplaced. For instance, Table 1 should be in Section 3, yet it appears before Section 2 in both files. There are additional instances of the same problem; please correct the placements in the final typeset version.

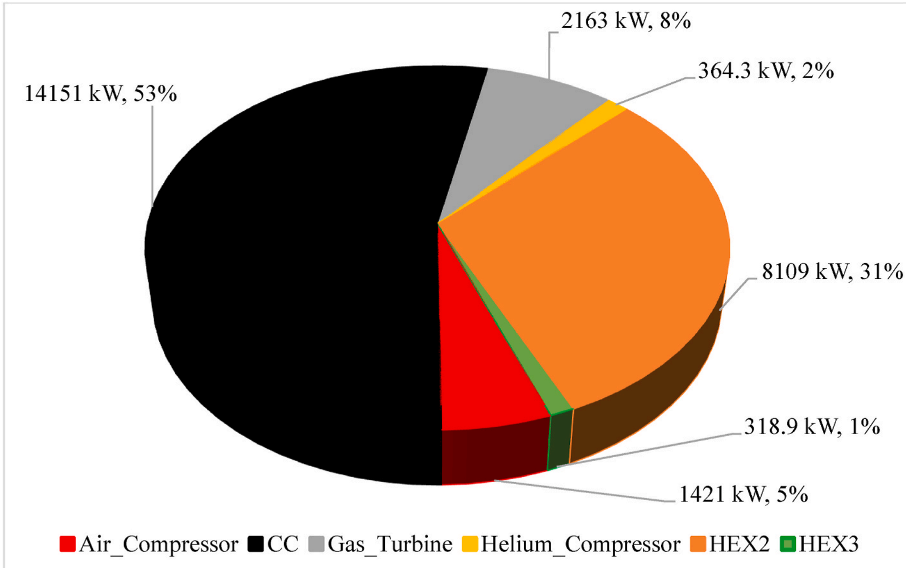

Fig. 12. Exergy destruction rates in proposed model.

%-4000 kW and 75.05 %-93.45 %-21,013 kW, respectively.

According to the thermodynamic analysis results, the total exergy destruction rate of the proposed model is calculated as 26,527 kW. As shown in the exergy destruction rates presented in Fig. 12, the highest exergy destructions occur in the combustion chamber at 53 % and in HEX-2 at 31 %. These values highlight the importance of optimization to minimize exergy losses.

Fig. 13 presents the distribution of fuel exergy in the overall power plant. The large amount of exergy lost with the exhaust gas in the ABP is recovered through the IESs. With the IESs, the highest recovered flow exergy belongs to HEX-2, corresponding to 74.18 % of the total fuel exergy. The flows shown in black represent exergy outputs from the system, while the flows shown in green indicate exergy inputs to the system. Independent of exergy destructions, reducing exergy outputs from the system is a crucial consideration in the design to enhance the system's exergy efficiency.

Table 2 presents the proposed model's unit flow costs, flow exergies, and flow exergy cost rates. According to the laws of thermoeconomics, the cost of a unit flow affects the costs of other connected flows. Therefore, the plant's electricity cost is critical in determining the product costs in processes such as hydrogen production, hydrogen liquefaction, and carbon dioxide liquefaction, where electricity is used. By reducing exergy losses, the cost of electricity and, consequently, the cost of products generated using electricity can be minimized.

The equipment purchase costs (EPC), equipment installation costs (EIC), and equipment cost rates (ECR) in the proposed model are presented in Table 3.

In order to evaluate the accuracy of the study, the thermodynamic

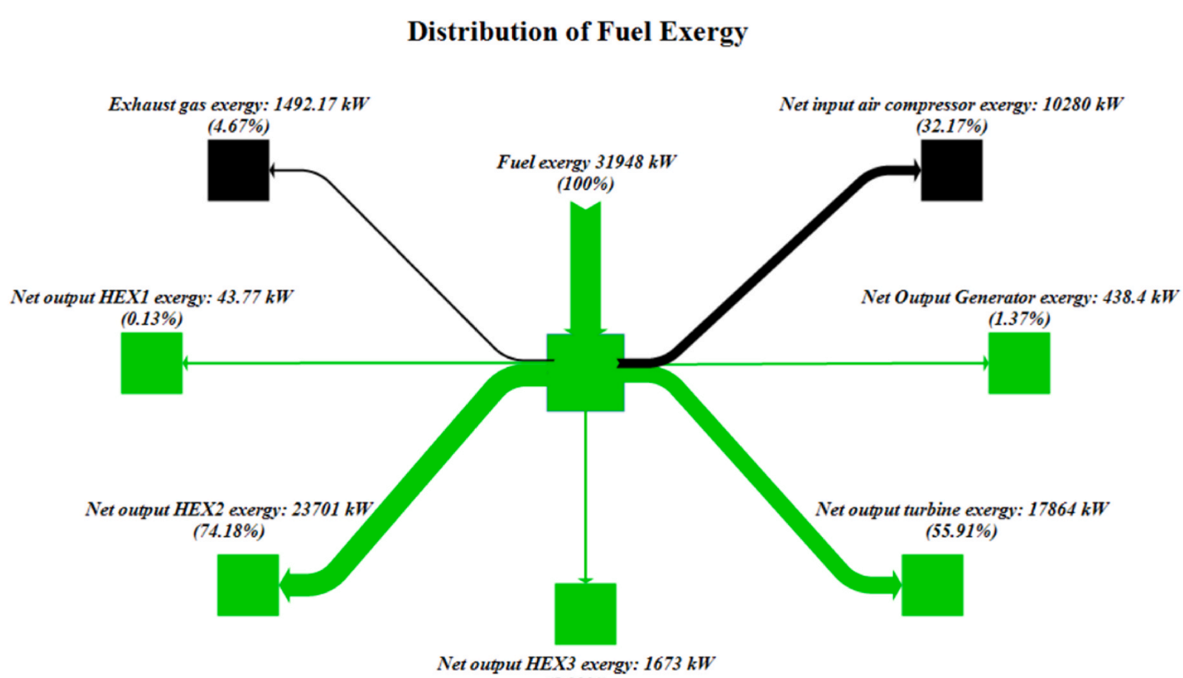

Fig. 13. Distribution of fuel exergy.

Table 2
Unit flow costs, flow exergies, and flow exergy cost rates of the proposed model.

State	Unit Flow Cost ($/GJ)	Flow Exergy (kW)	Flow Exergy cost rate ($/h)
1	0	0	0
2	24.35	10280	901.14
3	15.18	28077	1534.35
4	15.18	10213	558.12
5	15.18	10195	557.13
6	0	1882	0
7	0	1736	0
8	0	1358	0
9	0	0.000125	0
10	128.2	2.195	1.01
11	128.2	2.195	1.01
12	25500	1.48	135.86
13	22	169.4	13.41
14	22	5.944	0.47
15	44.95	24.18	3.91
16	44.95	48.98	7.92
17	44.95	80.67	13.05
18	44.95	173.3	28.04
19	23.6	39.37	3.34
20	23.6	0.000145	1.23E-05
21	1.23	257.3	1.14
22	5.272	712	13.51
23	5.272	990.3	18.79
24	41.16	1424	211
25	42.6	1376	211.02
26	42.6	1868	286.47
27	44.95	1771	286.58
28	45.52	1658	271.7
29	50.44	1077	195.56
30	1.639	560.8	3.31
31	5.875	10.34	0.21
32	1.058	8.396	0.03
33	1.058	10.73	0.04
34	1.186	142	0.6
35	1.186	94.5	0.83
36	1.478	196.7	1.04
37	0.051	277.7	0.05
38	0.07591	255.6	0.07
39	0.319	248.7	0.28
40	1.838	212.3	1.4
41	0	0.3992	0
42	121	28.45	12.39
43	143.7	24.19	12.51
44	99.12	55.91	19.95
45	86.47	70.04	21.8
46	0.6551	1.085	0.002
47	0.6551	60.1	0.14
Product		**Value**	
Electricity		65.7 $/MWh	
Hydrogen Production		2.64 $/kg	
Hydrogen Liquefaction		2.754 $/kg	
Liquid Hydrogen		5.394 $/kg	
Carbon dioxide Liquefaction		0.36 $/kg	
Hot Water		2.358 $/MWh	

Table 3
Equipment purchase, installation, and equipment cost rates for the proposed model.

Equipment	EPC ($)	EIC ($)	ECR ($/h)
Air_Compressor	12,260,000	12,971,200	132.3
CC	51,500	58,900	0.55
Gas Turbine	5,139,000	5,434,200	55.44
HEX-1	20,000	24,200	0.56
HEX-2	710,000	1,109,600	55.46
HEX-3	12,900	84,100	0.22
HEX-4	9100	67,000	7.66
HEX-5	77,400	196,100	0.14
HEX-6	344,500	1,165,000	0.10
HEX-7	395,300	1,339,200	0.84
HEX-8	10,600	155,200	3.72
Electrolyser	340,000	372,100	4.27
He_Compressor	1,733,500	1,893,200	0.11
He_Turbine_1	91,000	193,200	3.67
He_Turbine_2	90,700	221,100	18.71
Reactor	162,700	325,300	0.98
Purifier	16,500	128,000	0.98
Generator	47,700	49,900	1.76
Condenser	11,200	72,300	0.18
Expansion Valve-1	20,000	22,000	0.51
Evaporator	15,100	88,800	0.12
Absorber	468,600	684,200	0.22
Pump	17,300	45,100	0.16
Regenerator	27,500	78,400	5.06
Expansion Valve-2	20,000	22,000	0.19
Pretreatment	34,776	49,680	0.28
Total	**22,126,876**	**26,849,980**	**238.68**

Table 4
The validation of the proposed model.

	Thermodynamic Findings	Thermoeconomic Finding
[45]	68.4 % – energy efficiency 25.8 % – exergy efficiency	69.7 $/GJ – product cost
[113]	18.9 % – energy efficiency 16.9 % – exergy efficiency	325 $/GJ – product cost
[114]	76 % – energy ratio 21.56 % – exergy efficiency	50 $/GJ – product cost
[115]	33.33 % – exergy efficiency	57.7 $/GJ – hydrogen cost
Proposed model	75.05 % – energy efficiency 93.45 % – exergy efficiency	22 $/GJ – hydrogen cost

and thermoeconomic performance results of the system were validated by comparing them with similar studies in the literature. In this context, as presented in Table 4, the results obtained in the present study were compared with reference data by considering key performance parameters, and the consistency between them was analyzed. The comparisons carried out support that the model is valid, reliable, and highly efficient, indicating that the proposed system remains within acceptable limits in terms of design and analysis.

5. Conclusions

This study presents a high-efficiency multi-generation model for ABP, integrating various energy systems for heating, carbon dioxide liquefaction, hydrogen production and liquefaction, and hot water production. The thermodynamic and thermoeconomic analyses indicate a significant improvement in the plant's performance, with energy and exergy efficiencies increasing from 14.29 % to 12.52 %–75.05 % and 93.45 %, respectively. The proposed model effectively utilizes waste energy, reducing exergy losses and enhancing economic feasibility.

One of the focal points of the study is the coordinated use of EES and Aspen Plus software. EES is a coding program with a comprehensive thermodynamic database that includes numerous substances' thermophysical and thermochemical properties, allowing for the design of various thermodynamic processes. Similarly, Aspen Plus has a vast database and enables the simulation of many processes. It selects the most suitable equipment for the designed model and can retrieve all relevant economic data from the internet in real time. Since the proposed model involves biogas production, combustion, cooling, and heating processes, analyzing and simulating it within a single program is not feasible. The coordinated use of EES and Aspen Plus has realistically solved this problem.

Eventually, the proposed model enables cost-effective production by efficiently utilizing all beneficial and harmful byproducts produced during biogas production. No external energy input is needed since the proposed model generates all the energy required for this process. Besides, efficiently utilizing exhaust gas waste energy minimizes the thermal impact on the environment.

Although the study presents a biogas power plant model that produces economical and high-efficiency liquid hydrogen from biomass with high performance and in an environmentally friendly manner, it has several limitations.

- This model is designed based on the operating conditions and resource availability of the ABP operating in Afyon, which is located in a rural area of Turkey. Therefore, the model's applicability will be limited in regions with insufficient biomass resources or no existing biogas infrastructure.
- Although theoretically scalable, the system depends on site conditions such as regional feedstock potential, local energy demand, and legislation. In addition, initial investment costs of system components such as multiple production technologies, hydrogen liquefaction, and CO_2 capture may create economic difficulties in small-scale applications.
- Especially considering the equipment maintenance and the periodic acid rate of biogas, the decomposers of the plant cannot be employed with 100 % performance.
- Increasing the reactor temperature positively affects methane yield and produces more methane from the same amount of biomass. However, the use of all the produced methane in the combustion chamber is limited by the thermal resistance of the equipment and the risk of NOx formation.
- In order to increase the electrolysis efficiency, the water is heated before electrolysis, and the maximum temperature is 80°. This limitation has critical importance in terms of preventing the water from tending to evaporate before electrolysis.

For future studies, several aspects can be explored to optimize the system further.

- Advanced Optimization Techniques: Integrating artificial intelligence-based optimization algorithms could enhance system performance and cost-effectiveness.
- Experimental Validation: Conducting experimental studies to validate the simulation results and assess real-world operational feasibility.
- Alternative Working Fluids: Investigating different working fluids for the absorption and ORC systems to improve thermal efficiency.
- Energy Storage Solutions: Integrating thermal or chemical energy storage systems to balance supply and demand fluctuations.
- These aspects will contribute to the continuous improvement of integrated energy systems, making biogas power plants more efficient, cost-effective, and environmentally sustainable.
- A comprehensive life cycle assessment analysis can be done to evaluate the environmental sustainability of the proposed system.

Declaration of competing interest

The author declares that he has no known competing financial interests or personal relationships that could have appeared to influence the work reported in this paper.

Nomenclature

Abbreviations

ABP	Afyon Biogas Power Plant
CC	Combustion chamber
EES	Engineering equation solver
ECR	Equipment cost rate ($/h)
EIC	Equipment installation cost ($)
EPC	Equipment purchase cost ($)
HEX	Heat exchanger
HV	Heat value
IES	Integrated energy system
LNG	Liquid Natural Gas
NG	Natural Gas
PEM	Proton exchange membrane

Symbols

η	Efficiency (%)
c	Unit flow cost ($/MWh)
ex	Specific exergy (kJ/kg)
$\dot{Ex}$	Exergy (kW)
h	Specific enthalpy (kJ/kg)
ln	Natural Logarithm
$\dot{m}$	Mass flow rate (kg/hr)
P	Pressure (kPa)
$\dot{Q}$	Thermal power (kW)
R	Gas constant (kJ/kgK)
T	Temperature (K)
$\dot{W}$	Shaft Power (kW)
$\dot{Z}_k$	Total cost rate ($/h)

Subscripts

$dest$	Destroyed
en	Energy
ex	Exergy
f	Fuel
i	Input

isen Isentropic
o Output
p Product
rev Reversible

Appendix A. Supplementary data

Supplementary data to this article can be found online at https://doi.org/10.1016/j.ijhydene.2025.151333.

References

[1] Senol H. Estimation of biogas potential from poultry manure to 2040 in Türkiye using time series and the artificial neural network (ANN). Renew Sustain Energy Rev 2025;207:114976.
[2] Aigbe UO, Ukhurebor KE, Osibote AO, Hassaan MA, El Nemr A. Optimization and prediction of biogas yield from pretreated Ulva Intestinalis Linnaeus applying statistical-based regression approach and machine learning algorithms. Renew Energy 2024;235:121347.
[3] Godoy V, Martín-Lara MA, Garcia-Garcia G, Arjandas S, Calero M. Environmental impact assessment of the production of biomethane from landfill biogas and its use as vehicle fuel. Renew Energy 2024;237(Part B):121685.
[4] Calise F, Cappiello FL, Cimmino L, d'Accadia MD, Vicidomini M. Dynamic simulation and thermoeconomic analysis of a power to gas system. Renew Sustain Energy Rev 2023;187:113759.
[5] Kumawat R, Gidwani L, Rana KB. Comparative analysis of life cycle assessment of biogas-powered and coal-powered power plant for optimized environmental operation. Heliyon 2024;10:e39155.
[6] Aravindan M, Kumar GP. Optimizing novel green hydrogen production from solar and municipal solid waste: a thermo-economic investigation with environmental comparison between integrated low temperature power cycles. Process Saf Environ Prot 2024;186:421–47.
[7] Yağlı H, Koç Y, Köse Ö, Koç A, Yumrutaş R. Optimisation of simple and regenerative organic Rankine cycles using jacket water of an internal combustion engine fuelled with biogas produced from agricultural waste. Process Saf Environ Prot 2021;155:17–31.
[8] Liu J, Yang M, Chauhan BS, Abdrabboh M, Fayed M, Ayed H, Mouldi A, Chen Y, Chen X. A comparison of two schemes for pure hydrogen injection into a syngas-fueled SOFC: thermoeconomic and environmental-based investigations. Process Saf Environ Prot 2023;175:783–95.
[9] Wang L, Bo G, Gao R, Ayadi M, Chammam W, Ooi JB, Qin M. Thermoeconomic assessment of an innovative combined cooling, heating, and power system based on biomass combustion, TCO_2 cycle, absorption chiller, and desalination. Process Saf Environ Prot 2024;184:151–69.
[10] Pera L, Gandiglio M, Marocco P, Pumiglia D, Santarelli M. Trace contaminants in biogas: biomass sources, variability and implications for technology applications. J Environ Chem Eng 2024;12:114478.
[11] Negro V, Noussan M, Chiaramonti D. Alternative options for biogas-to-energy: a comparison of electricity and biomethane generation based on the real operation of a production site. Appl Energy 2025;377:124687.
[12] Mutunga JM, Ndiritu H, Hawi M, Oketch P. Experimental study of four-step thermal swing adsorption cycle to upgrade biogas obtained from anaerobic digestion. Energy Storage and Saving 2024;3:278–87.
[13] Sathish T, Muthukumar K, Saravanan R, Giri J. Optimized thermal pretreatment for lignocellulosic biomass of pigeon pea stalks to augment quality and quantity of biogas production. International Journal of Thermofluids 2024;24:100911.
[14] Abusoglu A, Tozlu A, Anvari-Moghaddam A. District heating and electricity production based on biogas produced from municipal WWTPs in Turkey: a comprehensive case study. Energy 2021;223:119904.
[15] Song Y, Ahmad SF, Houran MA, Agrawal MK, Nutakki TUK, Siddiqui MR, Albani A, Su Q. Multi-variable study of a novel multigeneration system using biogas separation unit and LNG cold energy utilization, producing electricity, cooling, heat, fresh water, liquid CO2, biomethane, and methanol. Process Saf Environ Prot 2023;180:616–38.
[16] Tian H, Chen X, Ahmad SF, Agrawal MK, Seikh AH, Shah NA, Su Q. Modeling and 4E analysis of a new combined cooling, heating, and power energy system based on biogas combustion and hot oil for heat supply. Process Saf Environ Prot 2024;184:1484–501.
[17] Yang K, He Y, Du N, Zhu N, Chen Y, Wang J, Lund PD, Cao L. Exergy and exergoeconomic analyses of multi-energy complementary system based on different natural gas and biogas co-firing ratios considering carbon tax. Process Saf Environ Prot 2024;184:1206–21.
[18] An M, Shen L, Liang R, Li Y, Zhao G. Microbial diagnostics unveil key driver bacteria and methanogens associated with system stability and biogas production in food waste anaerobic digestion systems. J Environ Chem Eng 2024;12:114435.
[19] Shen R, Sun P, Liu J, Luo J, Yao Z, Zhang R, Yu J, Zhao L. Robust prediction for characteristics of digestion products in an industrial-scale biogas project via typical non-time series and time-series machine learning algorithms. Chem Eng J 2024;498:155582.
[20] Ghorbani B, Ebrahimi A, Ziabasharhagh M. Thermodynamic and economic evaluation of biomethane and carbon dioxide liquefaction process in a hybridized system of biogas upgrading process and mixed fluid cascade liquefaction cycle. Process Saf Environ Prot 2021;151:222–43.
[21] Nitschke A, Hitzemann M, Winkelholz J, Kobelt T, Thoben C, Lippmann M, Stolpe L, Plinke H, Zimmermann S. Ultra-fast polarity switching GC-IMS for the analysis of volatiles in biogas. Renew Energy 2024;231:120941.
[22] Ravaei H, Pesteei SM. Efficiency enhancement of an actual wastewater treatment power plant by improving and redesigning heat exchangers. Process Saf Environ Prot 2025;195:106805.
[23] Liu J, Hsu CY, Ahmad SF, Alotaibi MA, Allahham MI, Qin M. Design and energy, exergy, thermoeconomic, and exergo-environmental (4E) analyses of a novel hybrid geothermal/biogas-powered green multi-generation system using a post-combustion CO2 capture unit. Appl Energy 2025;377:124662.
[24] Kimutai SK, Dushengere B, Muchilwa I. Assessing the viability of solar-biogas hybrid systems for energy provision in rural Kenyan communities. Sustain Energy Technol Assessments 2025;75:104244.
[25] Panbechi B, Hajinezhad A, Moosavian SF, Fattahi R. Enhancing the enviro-economic viability of biogas-solar hybrid systems: strategies for sustainable energy development in Iran. Energy Strategy Rev 2025;58:101671.
[26] Akbulut A. Energy, exergy and enviro-economic analysis of a hybrid energy plant utilizing biogas and solar technologies in the Almaty region, Republic of Kazakhstan. Case Stud Chem Environ Eng 2025;11:101118.
[27] Hüner B. Feasibility and environmental analysis of biogas-based hybrid energy system using HOMER pro software: a case study for Hatay. Energy Convers Manag 2025;326:119480.
[28] Rong Q, Shami HO, Ali ABM, Alshamrani A, Agarwal D, Ahmed M, Rajab H, Mabrouk A, Kolsi L, Said LB, El-Shafay AS. Environmental, financial, and technological viability of based on a Grid/PV/battery/wind/electrolyzer/biogas hybrid configuration for producing energy and hydrogen. Int J Hydrogen Energy 2025;103:836–50.
[29] Sun T, Chong WT, Khairuddin ASM, Tey KS, Wang X, Wu J, Pan S, Pang L. Design and performance evaluation of a solar-assisted biogas and air-source heat pump hybrid system for radiant heating applications. J Build Eng 2024;97:110944.
[30] Ran P, Ou YF, Zhang CY, Chen YT. Energy, exergy, economic, and life cycle environmental analysis of a novel biogas-fueled solid oxide fuel cell hybrid power generation system assisted with solar thermal energy storage unit. Appl Energy 2024;358:122618.
[31] Ennemiri N, Berrada A, Emrani A, Abdelmajid J, Mrabet RE. Optimization of an off-grid PV/biogas/battery hybrid energy system for electrification: a case study in a commercial platform in Morocco. Energy Convers Manag X 2024;21:100508.
[32] Nguyen VG, Sharma P, Bora BJ, Bui TMT, Efremov C, Tran MH, Kowalski J, Osman SM, Cao DM, Dong VH. Techno-economic analysis of a hybrid energy system for electrification using an off-grid solar/biogas/battery system employing HOMER: a case study in Vietnam. Process Saf Environ Prot 2024;191:1353–67.
[33] Emrani A, Berrada A. Modeling and optimal capacity configuration of dry gravity energy storage integrated in off-grid hybrid PV/Wind/Biogas plant incorporating renewable power generation forecast. J Energy Storage 2024;97:112698.
[34] Jaman A, Das BK, Mahim M, Hasan A, Siddika S, Ahmed MM, Okonkwo PC. Techno-econo-environmental analysis of sustainable hybrid solar-wind-biogas using municipal solid waste-based grid independent power plant with dual mode energy storage strategy. Energy 2024;307:132777.
[35] Nassereddine M, Nassreddine G, Arid AE. Hybrid photovoltaic and biogas system for stable power system. Next Energy 2024;5:100172.
[36] Mukhtar S, Muhammad S, Alyousef HA, Khan W, Shah R, El-Tantawy SA. Enviro-economic and optimal hybrid energy system: photovoltaic–biogas–hydro–battery system in rural areas of Pakistan. Heliyon 2024;10:e35182.
[37] Mei B, Li R, Wang Y, Qing Y. Comprehensive 4E analysis and optimization of a hybrid solar-biogas gas turbine system Coupled with a geothermal flash cycle for hydrogen and freshwater production. Int J Hydrogen Energy 2025;105:56–79.
[38] Zahedi A, Rasmi E, Ahmadi A, Kanani B. Conceptual design of a novel sustainable hybrid renewable energy system based on biogas/molten carbonate fuel cell/water desalination for a building energy supply. Renew Energy 2024;237:121749.
[39] Pan J, Bai J, Zhang G, Gao X. Proposing an innovative polygeneration process based on biogas fuel: a comprehensive thermo-enviro-economic (4E) analysis. Energy 2024;304:132157.
[40] Cimmino L, Burgos JB, Eicker U. Exergy and thermoeconomic analysis of a novel polygeneration system based on gasification and power-to-x strategy. Renew Energy 2024;236:121438.
[41] Atak YN, Ince AC, Colpan CO, Iulianelli A, Serincan MF, Pasaogullari U. Thermoeconomic analysis of an integrated membrane reactor and carbon dioxide capture system producing decarbonized hydrogen. Energy Convers Manag 2025;326:119506.

[42] Abouzied AS, Samad S, Abed AM, Shaban M, Alhomayani FM, Shomurotova S, Safi MS, Ghandour R, Elmasry Y, Alrawashdeh AI. Efficient thermal integration model based on a biogas-fired gas turbine cycle (GTC) for electricity and desalination applications; thermo-economic and GA-based optimization. Case Stud Therm Eng 2024;64:105492.
[43] Wang M, Ahmad SF, Agrawal MK, Ahmad AYAB, Awan AB, Usmani YS, Chauhdary ST, Han W. Thermodynamic, economic, and environmental footprint assessments and optimization of an innovative biogas-driven heat integration network, producing power, cooling, and heating. Energy 2025;322:135379.
[44] Wu Y, Xu Y. Comprehensive evaluation of an environmentally friendly multi-heat recovery system using biogas energy source from thermodynamic, economic, and environmental perspectives. J Environ Chem Eng 2024;12:112783.
[45] Zhang J, Alotaibi MA, Wang M. Thermo-enviro-economic analyses of a landfill biogas-fed polygeneration process combined with a liquefied natural gas cold energy utilization unit. Appl Therm Eng 2024;257:124325.
[46] Calise F, Cappiello FL, Cimmino L, d'Accadia MD, Vicidomini M. Dynamic analysis and thermoeconomic optimization of a Power-to-Gas system driven by renewables. Energy Convers Manag 2024;313:118647.
[47] Wu Y. Thermoeconomic modeling of new energy system based on biogas upgrading to multigenerational purpose. Desalination 2025;593:118215.
[48] Chatterjee B, Mazumder D. Valorization of fruit and vegetable waste in a novel three-stage hybrid anaerobic digester for enhanced biogas production: performance study and microbial community analysis. Biochem Eng J 2024;209:109403.
[49] Kan KW, Chan YJ, Tiong TJ, Lim JW. Maximizing biogas yield from palm oil mill effluent (POME) through advanced simulation and optimisation techniques on an industrial scale. Chem Eng Sci 2024;285:119644.
[50] Cossel MV, Lewin E, Lewandowski I, Jablonowski ND. Energy yield decline of *Sida hermaphrodita* harvested for biogas production. Renew Sustain Energy Rev 2024;190:114069.
[51] Chen X, Liu W, Zhao Y, He H, Ma J, Cui Z, Yuan X. Optimization of semi-continuous dry anaerobic digestion process and biogas yield of dry yellow corn straw: based on "gradient anaerobic digestion reactor". Bioresour Technol 2023;389:129804.
[52] Okwu MO, Oyejide OJ, Oyekale J, Ezekiel K, Mawared C, Orikpetee OF, Okonkwo CP. Application of fuzzy mamdani model for biogas yield prediction in anaerobic Co-digestion of decomposable wastes. Procedia Comput Sci 2024;232:2259–68.
[53] Farzin F, Moghaddam SS, Ehteshami M. Auto-tuning data-driven model for biogas yield prediction from anaerobic digestion of sewage sludge at the south-tehran wastewater treatment plant: feature selection and hyperparameter population-based optimization. Renew Energy 2024;227:120554.
[54] Liu C, Nie X, Wang Z, Yang H, Wang J, Zhang H, Fan Y, He L, El-Badri AM, Batool M, Wang J, Kuai J, Wang B, Zhou G. Biogas slurry: a potential substance that synergistically enhances rapeseed yield and lodging resistance. Ind Crops Prod 2024;222:119643.
[55] Hickmann FMW, Salahshournia B, Andretta I, Létourneau-Montminy MP, Rajagopal R. Impact of lowering nitrogen content in pig manure through low crude protein diets on anaerobic digestion process stability, biogas yields, and digestate composition. Sci Total Environ 2024;953:175957.
[56] Mamimin C, O-Thong S, Reungsang A. Enhancing biogas production from hemp biomass residue through hydrothermal pretreatment and co-digestion with cow manure: Insights into methane yield, microbial communities, and metabolic pathways. J Environ Manag 2024;370:123039.
[57] Zavala VR, Pereira IB, Vieira RS, Aires FIS, Dari DN, Félix JHS, Lima RKC, Santos JCS. Challenges and innovations in green hydrogen storage Technologies. Int J Hydrogen Energy 2025;113:322–39.
[58] Sarsar L. Green hydrogen impact on economic growth: a cross-sectional analysis of 29 European countries. Renew Energy 2025;246:122898.
[59] Chowdhury P, Das P, Yeassin R, Agyekum EB, Al-Maaitah MI, Odoi-Yorke F. Exploring the potential of solar and wind-powered green hydrogen: production, costs and environmental impacts in South Asia. Int J Hydrogen Energy 2025;137:288–302.
[60] Nagel NO, Jåstad EO. Blue and green hydrogen–An analysis of competing pathways and their impact on the European energy system. Energy 2025;323:135898.
[61] Oroya LA, Cortez JC, Terada LZ, Silva JAA, Rider MJ. Distributionally robust optimization for green hydrogen plant planning considering extreme scenarios. Int J Hydrogen Energy 2025;133:112–23.
[62] Su R, Xiao Y, Hamza F, Mamadiyarov Z, Wahab A. Scaling up green hydrogen in China: economic opportunities and challenges. Int J Hydrogen Energy 2025;131:60–9.
[63] Li C, Hao Q, Zhang W, Wang S, Yang J. Development strategies for green hydrogen, green ammonia, and green methanol in transportation. Renew Energy 2025;246:122904.
[64] Sakthimurugan V, Lakshmikanth G, Balaji N, Roopashree R, Kumar D, Devarajan Y. Green hydrogen revolution: Advancing electrolysis, market integration, and sustainable energy transitions towards a net-zero future. Results Eng 2025;26:104849.
[65] Ma Y, Huang M, Zhou Y, Xu F, Xu C. Modeling of the multi-period two-stage green hydrogen supply chain with consideration of supply and demand uncertainties. Int J Hydrogen Energy 2025;129:297–314.
[66] Yin Z, Tang X, Li X. Multi-storage, multi-energy, and multi-policy optimization for hybrid green and grey hydrogen production: a regional study in China. Energy Convers Manag 2025;334:119784.
[67] Habour RM, Benyounis KY, Carton JG. Green hydrogen production from renewable sources for export. Int J Hydrogen Energy 2025;128:760–70.
[68] Selvam DC, Devarajan Y, Raja T, Vickram S. Advancements in water electrolysis technologies and enhanced storage solutions for green hydrogen using renewable energy sources. Appl Energy 2025;390:125849.
[69] Anand C, Chandraja B, Nithiya P, Akshaya M, Tamizhdurai P, Shoba G, Subramani A, Kumaran R, Yadav KK, Gacem A, Bhutto JK, Alreshidi MA, Alam MW. Green hydrogen for a sustainable future: a review of production methods, innovations, and applications. Int J Hydrogen Energy 2025;111:319–41.
[70] Chahtou A, Taoussi B. Techno-economic of solar-powered desalination for green hydrogen production: Insights from Algeria with global implications. Int J Hydrogen Energy 2025;121:210–27.
[71] Oni BA, Sanni SE, Misiani AN. Green hydrogen production in offshore environments: a comprehensive review, current challenges, economics and future-prospects. Int J Hydrogen Energy 2025;125:277–309.
[72] Hazem AEM, Zoghby HEM, Bendary AF, Afia RSA. Techno-economic study of a 100 % renewable energy-based isolated microgrid involving green hydrogen production. Sustain Energy Technol Assessments 2025;76:104303.
[73] Bag S, Routray S, Rahman MS, Shrivastav SK. Investigate the effect of green hydrogen supply chain integration on supply chain resilience: Organization information processing theory perspective. Int J Prod Econ 2025;284:109613.
[74] Haoxin D, Qiyuan D, Chaojie L, Nian L, Zhang W, Hu M, Xu C. A comprehensive review on renewable power-to-green hydrogen-to-power systems: green hydrogen production, transportation, storage, re-electrification and safety. Appl Energy 2025;390:125821.
[75] Cardinali VBA, de Souza TAZ, da Costa RBR, Pinto GM, Roque LFA, Vidigal LPV, Frez GV, Pérez-Rangel NV, Coronado CJR. Exploring possible pathways for green hydrogen-based transportation in Brazil: fuel cells, hydrogen engines and dual-fuel combustion. Int J Hydrogen Energy 2025;120:238–53.
[76] Yang j, Fu B, Peng J, Wang G, Yao H. Integration of a salt cavern for large-scale hydrogen storage into a solar-wind-storage power system: Technical and economic advantages. Appl Energy 2025;393:126073.
[77] Pan Y, Yang F. Investigation of structural, hydrogen storage mechanism, electronic and optical properties of B10N2H18-type hydrides for hydrogen storage. Chem Phys Lett 2025;872:142151.
[78] Liu S, Wu Z, Zhao S, Huang P, Liu D, Wang Y, Zhou Z, Wang J. A review on Mg-based materials for hydrogen storage tanks: development and mechanism. Int J Hydrogen Energy 2025;135:121–45.
[79] Xu J, Xu Y, Hu H, Zhang T, Liu K, Huang Y, Guo Y, Zou J, Liu Y, Chen Q. Effect of Co content on microstructure evolution and hydrogen storage properties of La0.6Y0.15Ca0.9Mg1.05Ni9Co*x* alloys. J Energy Storage 2025;122:116714.
[80] Pan Y, Zhu Y. Theoretical prediction of novel phase, phonon dynamics and physical properties of KAlH4 hydride for hydrogen storage. Int J Hydrogen Energy 2025;131:221–8.
[81] Sun Y, Zhao B, Han J, Li B, Zhang C, Gao P. Exploration of Li-decorated g-C2O monolayer for enhancing hydrogen storage via first-principles calculations. Int J Hydrogen Energy 2025;138:344–51.
[82] Qiuchen Z, Ping Z, Xiqiang Z. Challenges and opportunities of microwave technology in hydrogen production, storage and utilization: a review. Int J Hydrogen Energy 2025;134:283–98.
[83] Yang J, Lam TY, Luo Z, Cheng Q, Wang G, Yao H. Renewable energy driven electrolysis of water for hydrogen production, storage, and transportation. Renew Sustain Energy Rev 2025;218:115804.
[84] Zohri M, Suwarno S, Haryadi H, Fudholi A. Review of hydrogen storage sustainability using bibliometric and mathematical modeling analysis. J Energy Storage 2025;123:116710.
[85] Zhang J, Sander R, Heryanto D, Clennell MB. Hydrogen storage capacity in clay: an analytical model for storage density as a function of pore size, pressure, and temperature. Fuel 2025;398:135460.
[86] Zaman M, Zafar S, Zeba I, Gillani SSA. DFT assessment of KBeO3-xHx perovskites: Revealing ion substitution mechanisms for enhanced solid hydrogen storage. Int J Hydrogen Energy 2025;138:307–19.
[87] Zhang X, Abid I. Cost-effective hydrogen transport: analyzing the economics of hydrogen storage systems. Int J Hydrogen Energy 2025;137:360–6.
[88] Zhang Z, Ma K, Li L, Peng W, Zheng J. Study on the quenching strategies for seamless hydrogen storage vessels made of Cr–Mo steel. Int J Hydrogen Energy 2025;124:280–9.
[89] Altaf M, Demirci UB, Haldar AK. Review of solid-state hydrogen storage: materials categorisation, recent developments, challenges and industrial perspectives. Energy Rep 2025;13:5746–72.
[90] Hua Z, Gao W, Chi S, Wang X, Zheng J. Development status and challenges of high-pressure gaseous hydrogen storage vessels and cylinders in China. Renew Sustain Energy Rev 2025;214:115567.
[91] Liu H, Lei Y, Tan KC, Wang Y, ju X, Chu H, Zou Y, He T, Chua YS. Enhanced hydrogen storage through the synergistic integration of LiAlH4 and carbazole-based liquid organic hydrogen carrier. Int J Hydrogen Energy 2025;120:276–81.
[92] Lee MG, Kim S, Lee Y. Direct seawater electrolysis: Breaking the dependency on noble metal-based electrocatalysts. Int J Hydrogen Energy 2025;130:89–107.
[93] Puteanus S, Miličić T, Feldmann U, Vidaković-Koch T. Efficiency improvement by pulsed water electrolysis: an unjustified hope. Int J Hydrogen Energy 2025;113:478–84.
[94] Zignani SC, Salanitro A, Pascale M, Fazio M, Arico AS. Cell preservation strategies in direct seawater electrolysis based on cost-effective anion exchange membrane technology. Electrochim Acta 2025;530:146406.

[95] Cao R, Wang Y, Li W, Ni H, Duan Y. Thermodynamics analysis of a hybrid system based on a combination of hydrogen fueled compressed air energy storage system and water electrolysis hydrogen generator. Int J Hydrogen Energy 2023;48:24492–503.
[96] Alkoshab MQ, Shaikh N, Qamar M, Toor IU. Innovations in seawater electrolysis: from fundamental challenges to practical applications. Int J Hydrogen Energy 2025;122:289–331.
[97] Sun J, Etcheverry L, Bergel A. Water electrolysis at near-neutral pH: a semi-empirical modelling strategy to assess the benefit of pressure on cell voltage. Electrochim Acta 2025;530:146264.
[98] Liu L, He D, Pan F, Huang R, Lin H, Zhang X. Comparative study on treatment of methylene blue dye wastewater by different internal electrolysis systems and COD removal kinetics, thermodynamics and mechanism. Chemosphere 2020;238:124671.
[99] Min G, Choi S, Hong J. A review of solid oxide steam-electrolysis cell systems: thermodynamics and thermal integration. Appl Energy 2022;328:120145.
[100] Li Q, Khosravi A, Farsaei A, Sun L. Thermodynamics, economic and carbon emission analysis of power-to-methanol process through alkaline electrolysis and monoethanolamine (MEA) carbon capture. Chem Eng Sci 2024;293:120029.
[101] Li Y, Zhang Q, Li Y, Xu Y, Li L, Tian D. Improving the efficiency of seawater desalination and hydrogen production: challenges, strategies, and the future of seawater electrolysis. Desalination 2025;609:118882.
[102] Ma Y, Xi S, Li X, Li J, Tao C, Liu Z. Fe3+-mediated coal-assisted water electrolysis for hydrogen production: evolution of coal structure oxidation via direct current and chaotic electric fields. Energy 2025;322:135590.
[103] Ebadollahi M, Rostamzadeh H, Pourali O, Ghaebi H, Amidpour M. Inherently safety design of a dual-loop bi-evaporator combined cooling and power system: 4E and safety based optimization approach. Process Saf Environ Prot 2021;154:393–409.
[104] Dai H, Li Z, Wang X, Gao X. Thermal enhanced porous media for the efficient partial oxidation of methane to produce hydrogen-rich syngas: Effects of heat conductive parameter and packed bed structure. Powder Technol 2025;461:121107.
[105] Köse Ö, Koç Y, Yağlı H. Performance improvement of the bottoming steam Rankine cycle (SRC) and organic Rankine cycle (ORC) systems for a triple combined system using gas turbine (GT) as topping cycle. Energy Convers Manag 2020;211:112745.
[106] Scaccabarozzi R, Tavano M, Invernizzi CM, Martelli E. Comparison of working fluids and cycle optimization for heat recovery ORCs from large internal combustion engines. Energy 2018;158:396–416.
[107] Gholizadeh T, Vajdi M, Rostamzadeh H. Exergoeconomic optimization of a new trigeneration system driven by biogas for power, cooling, and freshwater production. Energy Convers Manag 2020;205:112417.
[108] Hosseini SE, Wahid MA. Development of biogas combustion in combined heat and power Generation. Renew Sustain Energy Rev 2014;40:868–75.
[109] Benaissa S, Adouane B, Ali SM, Mohammad A. Effect of hydrogen addition on the combustion characteristics of premixed biogas/hydrogen-air mixtures. Int J Hydrogen Energy 2021;46:18661–77.
[110] Nadaleti WC, Przybyla G, Filho PB, de Souza SNM, Quadro M, Andreazza R. Methaneehydrogen fuel blends for SI engines in Brazilian public transport: potential supply and environmental issues. Int J Hydrogen Energy 2017;42:12615–28.
[111] Ghosh A, Sharma T, Pandey J. Review on proton conducting membrane for PEM water electrolyser: a sustainable approach for green hydrogen production. J Electroanal Chem 2025;993:119286.
[112] Feng Q, Yuan XZ, Liu G, Wei B, Zhang Z, Li H, Wang H. A review of proton exchange membrane water electrolysis on degradation mechanisms and mitigation strategies. J Power Sources 2017;366:33–55.
[113] Farhang B, Ghaebi H, Javani N. Techno-economic modeling of a novel poly-generation system based on biogas for power, hydrogen, freshwater, and ammonia production. J Clean Prod 2023;417:137907.
[114] Madhesh K, Devesh DR, Vivin T, Raj MP, Phelan PE, Kumar VV, Kumar GP. Analysis and multi-objective evolutionary optimization of Solar-Biogas hybrid system operated cascade Kalina organic Rankine cycle for sustainable cooling and green hydrogen production. Energy Convers Manag 2024;301:117999.
[115] Gholizadeh T, Ghiasirad H, Skorek-Osikowska A, Arabkoohsar A. Techno-economic optimization and working fluid selection of a biogas-based dual-loop bi-evaporator ejector cooling cycle involving power-to-hydrogen and water facilities. Int J Hydrogen Energy 2024;76:247–62.